Applied Physics Letters

Enhanced intrinsic piezoelectric response in (001)-epitaxial single c-domain $Pb(Zr,Ti)O_3$ nanorods

Cite as: Appl. Phys. Lett. **117**, 042905 (2020); https://doi.org/10.1063/5.0012998
Submitted: 07 May 2020 . Accepted: 18 July 2020 . Published Online: 30 July 2020

Kazuki Okamoto, Tomoaki Yamada, Kentaro Nakamura, Hidenori Takana, Osami Sakata, Mick Phillips, Takanori Kiguchi, Masahito Yoshino, Hiroshi Funakubo, and Takanori Nagasaki

Applied Physics Letters ARTICLE scitation.org/journal/apl

Enhanced intrinsic piezoelectric response in (001)-epitaxial single *c*-domain Pb(Zr,Ti)O_3 nanorods

Cite as: Appl. Phys. Lett. **117**, 042905 (2020); doi: 10.1063/5.0012998
Submitted: 7 May 2020 · Accepted: 18 July 2020 ·
Published Online: 30 July 2020

Kazuki Okamoto,[1] Tomoaki Yamada,[1,2,3,a)] Kentaro Nakamura,[1] Hidenori Takana,[3] Osami Sakata,[4] Mick Phillips,[5] Takanori Kiguchi,[6] Masahito Yoshino,[1] Hiroshi Funakubo,[3,7] and Takanori Nagasaki[1]

AFFILIATIONS

[1]Department of Energy Engineering, Nagoya University, Furo-cho, Chikusa-ku, Nagoya 464-8603, Japan
[2]PRESTO, Japan Science and Technology Agency, Kawaguchi 332-0012, Japan
[3]Department of Innovative and Engineered Material, Tokyo Institute of Technology, Yokohama 226-8503, Japan
[4]Synchrotron X-ray Group and Synchrotron X-ray Station at SPring-8, National Institute for Materials Science, 1-1-1 Kouto, Sayo, Hyogo 679-5148, Japan
[5]Micron Oxford, Department of Biochemistry, University of Oxford, Oxford OX1 3QU, United Kingdom
[6]Institute for Materials Research, Tohoku University, Sendai, Miyagi 980-8577, Japan
[7]School of Materials and Chemical Technology, Tokyo Institute of Technology, Yokohama 226-8502, Japan

[a)]**Author to whom correspondence should be addressed:** t-yamada@energy.nagoya-u.ac.jp

ABSTRACT

In this study, (001)-epitaxial tetragonal phase Pb(Zr, Ti)O_3 (PZT) nanorods were fabricated on $SrRuO_3/SrTiO_3$ substrates by pulsed laser deposition. The PZT nanorods were self-assembled and grown on the substrate at an elevated oxygen pressure, and showed a complete *c*-domain structure. Time-resolved x-ray diffraction measurements under an applied electric field show that the fabricated PZT nanorods exhibit a piezoelectric constant, d_{33}, that is significantly higher than that of thin PZT films and comparable to that for unclamped single-domain bulk crystals, which is thought to be due to a significant reduction in substrate clamping. The obtained results demonstrate that the self-assembled nanorods can achieve an enhanced intrinsic piezoelectric response, which makes them attractive for a range of practical applications.

Ferroelectric materials, particularly Pb(Zr, Ti)O_3 (PZT), have been utilized in various electromechanical devices due to their superior piezoelectric properties. The piezoelectric response of ferroelectric materials can be broadly classified into intrinsic and extrinsic responses. The intrinsic contribution is associated with increasing the magnitude of polarization within ferroelectric domains by an applied field, and the extrinsic response involves the movement of domain walls as the applied field induces reorientation of the polarization vector within domains. With the rapid growth in applications of microelectromechanical systems that utilize miniaturized ferroelectric materials on substrates, controlling the intrinsic and extrinsic responses in such small-scale materials has become increasingly important.[1]

In the case of thin films, substrate clamping is known to be a dominant factor in both the intrinsic and extrinsic responses. For example, it is widely known that the intrinsic piezoelectric response is suppressed by substrate clamping,[1–4] except under certain specific circumstances.[5] The extrinsic response is often suppressed by substrate clamping as well, though some reports have shown improved extrinsic contributions from clamping via domain engineering.[6,7]

Due to significantly different mechanical boundary conditions relative to thin films, nanostructures with a high aspect ratio, such as nanorods and nanoislands, grown on substrates may exhibit reduced clamping effects, enabling intrinsic contributions to approach those of unclamped single crystals. The extrinsic response should also increase, though to a lesser degree due to the lack of a mechanical restoring force. Among important pioneering works,[8–14] for example, Nagarajan *et al.* demonstrated a larger piezoelectric response in a Pb($Zr_{0.2}Ti_{0.8}$)O_3 nanoisland shaped by focused ion beam (FIB) compared with that in films.[10,11] Nguyen *et al.* fabricated Pb($Zr_{0.52}Ti_{0.48}$)O_3 nanorods of varying lengths with near morphotropic phase boundary composition using pulsed laser deposition (PLD) and showed that the longer PZT nanorods displayed a larger piezoelectric response.[14] Both these findings can be explained by a reduction in substrate clamping in the high aspect

ratio structures. However, the reduction of substrate clamping in such structures often varies the domain structure too,[9] complicating the quantitative estimation of the response increase caused by reduced substrate clamping effects.

Here, we demonstrate a piezoelectric constant, d_{33}, in self-assembled (001)-tetragonal phase PZT nanorods, as high as that in unclamped single-domain crystals. We suggest that this high value arises due to stabilization of the complete *c*-domain structure through an imperfect charge screening on the sidewall of the nanorods, coupled with a significant reduction in substrate clamping due to the high aspect ratio of the nanorods.

$Pb(Zr_{0.35}Ti_{0.65})O_3$ nanorods were fabricated at 600 °C in 2 Torr O_2 environment on $SrRuO_3/SrTiO_3$ (001) substrates by PLD using a fourth harmonic of Nd:YAG laser ($\lambda = 266$ nm), with a laser energy density of 0.44 J/cm^2 and a repetition rate of 10 Hz. The oxygen pressure employed was around 10 times greater than that typically used in the growth of thin films.[5] A higher oxygen pressure has been shown to promote the formation of PZT nanorods due to the enhanced shadowing effect, where the PLD species are frequently scattered, thereby increasing the population of PLD species having greater incident angles with respect to the substrate.[15] The PLD species with large incident angles predominantly arrive at the top of the islands formed on the growing surface. By continuing the deposition, the islands start to become isolated from each other and finally form nanorods. Note that the difference in laser source between the present and previous studies[15] does not cause significant difference in the nanorod growth conditions.

Prior to PZT deposition, 50 nm thick $SrRuO_3$ electrodes were grown epitaxially, through deposition by rf magnetron sputtering at 700 °C in 200 mTorr O_2.[16] Following PZT deposition, circular Pt top electrodes of 107 ± 12 or 207 ± 14 μm diameter were fabricated by electron beam evaporation using a through mask.

The structural properties of the fabricated PZT nanorods were characterized by x-ray diffraction (XRD) using a four-axis diffractometer with x-rays from Cu–$K\alpha_1$ (Bruker, D8 Discover) and synchrotron sources (SPring-8, BL13XU, and BL15XU beamlines) and transmission electron microscopy (TEM) (JEOL, JEM-3100F). TEM was also used for the chemical composition analysis. Surface morphology was observed by atomic force microscopy (Asylum research, Cypher). A precision LCR meter (Agilent Technologies, E4980A) and ferroelectric tester (Toyo, FCE-1) were used to measure the dielectric and ferroelectric properties of the PZT nanorods. Piezoelectric properties were measured by piezoelectric force microscopy (PFM) (Asylum research, Cypher) and XRD through the application of an electric field. The latter was employed to precisely characterize the nanorods' intrinsic piezoelectric constant to reveal the change in the lattice constant with applied field. This measurement was conducted using a time-resolved synchrotron XRD system with x-rays of 12.4 keV photon energy established at SPring-8, as described elsewhere.[17] The effective piezoelectric constant, d_{33}, was estimated from the change in the out-of-plane PZT (002) lattice spacing of the nanorods through the application of 200-ns-width voltage pulses.

The fabricated PZT nanorods showed a perovskite phase without any secondary phases, and the average Zr:Ti ratio was characterized to be 35.1:64.9, which is almost the same as that of nominal composition (see Fig. S1). The detailed structural properties of the fabricated PZT nanorods are shown in Fig. 1. As shown in Figs. 1(a) and 1(b), the

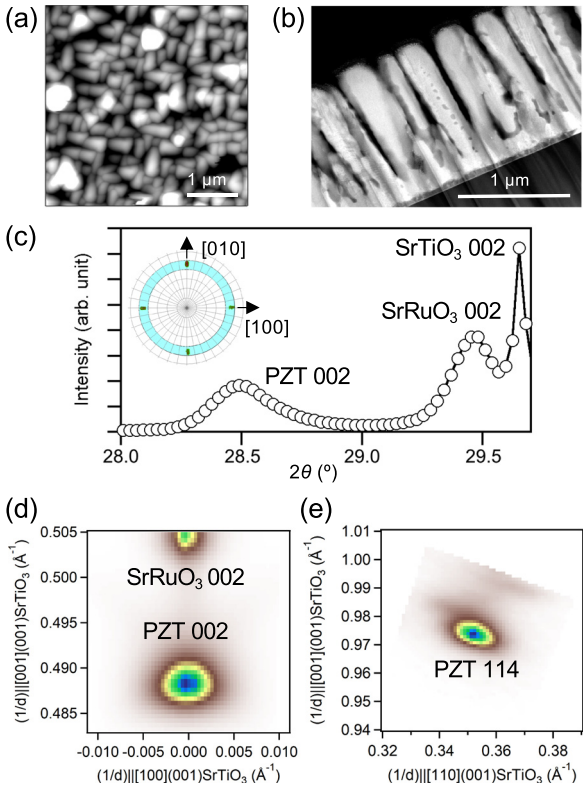

FIG. 1. Structural properties of the fabricated Pb(Zr, Ti)O_3 (PZT) nanorods: (a) surface morphology by atomic force microscopy, (b) cross-sectional transmission electron microscopy image, (c) x-ray diffraction (XRD) $2\theta/\omega$ scan and pole figure for PZT 101 (blue highlight indicates the scanned range), and (d) and (e) XRD reciprocal space maps around PZT 002/200 and PZT 114.

PZT produced a continuous layer of approximately 250 nm thick in the initial growth stage before forming into self-assembled nanorods. Continuous nanorod growth was achieved until the total thickness reached 1350 nm. The density of the nanorods was estimated to be in the range of 55%–60% from the surface and cross-sectional images. The PZT nanorods were epitaxially grown with a $\{001\}_{pc}$-orientation having a cube-on-cube relationship, as shown in Fig. 1(c). Similar epitaxial growth behavior was observed in our previous study on {111} PZT nanorods on $SrTiO_3$ (111) substrates,[15] which indicates that self-assembled epitaxial nanorod growth according to the substrate orientation can be achieved by PLD at an oxygen pressure higher than that typically used for the film growth.

A unique feature of the fabricated $\{001\}_{pc}$-epitaxial PZT nanorods was their domain structure. As shown in XRD reciprocal space map around PZT 002 and 200 [Fig. 1(d)], the nanorods showed XRD intensity for PZT 002 but not for PZT 200. In addition, from XRD reciprocal space map for PZT 114 [Fig. 1(e)], the in-plane and out-of-plane lattice constants of PZT were estimated to be 4.014 Å and 4.109 Å, respectively. Those results indicate that the nanorods are in a tetragonal phase (the same as bulks) and have the complete *c*-domain (without *a*-domains). The formation of the complete *c*-domain structure can be understood in terms of the depolarization field in nanorods.[19] Compared with the *c*-domain, in which polarization exists

along the longitudinal axis of the nanorod, the *a*-domain, with polarization perpendicular to the longitudinal axis, will undergo a significantly larger depolarization field due to the imperfect charge screening on the sidewall. For this reason, the *c*-domain will be more thermodynamically stable in this system. Stabilization of the *c*-domain in PZT nanorods of the same Zr:Ti composition as the present study has been reported elsewhere as a function of nanorod aspect ratio defined by FIB patterning,[18,19] which found that the complete *c*-domain structure can be obtained when the aspect ratio is larger than 1. The average and standard deviation of diameter of self-assembled nanorods in the present study were 166 and 70 nm, respectively (Fig. S2). Considering the three standard deviations, we can see that the most of nanorods have the aspect ratio greater than 2.9. Therefore, it is sufficiently larger than 1 required to obtain the complete *c*-domain structure.

Figure 2(a) shows the typical polarization-electric field (*P-E*) hysteresis loop for the (001)-PZT nanorods. The bars represent the possible error in the measurement of electrode size. It shows a well-saturated hysteresis, although its squareness is less pronounced compared to that observed in the epitaxial films.[20] It is also worth mentioning that the leakage current density below 250 kV/cm was smaller than 10^{-6} A/cm^2 (not shown here). Taking into account the density of the nanorods, the spontaneous polarization of the nanorods can be estimated to be in the range of 40–68 μC/cm^2. Although the uncertainty of spontaneous polarization estimated for the nanorods is large, given the nanorod morphology and measurement technique, the theoretical value of spontaneous polarization for the unclamped single crystal, 61 μC/cm^2,[21] is within this range. Figures 2(b) and 2(c) show the typical phase and amplitude of the piezoresponse in the single nanorod measured by PFM. It can be seen that even a single nanorod clearly demonstrates reversal polarization switching, i.e., ferroelectricity, and appreciable piezoelectric property. The details are found in Fig. S3. Although the statistically proven PFM analysis of the present nanorods remains challenging, the future comprehensive investigation of the nanorods with different size and domain structure would give deeper insight, as reported for other PZT nanostructures in literature.[10,12]

To accurately evaluate the intrinsic piezoelectric response, time-resolved synchrotron XRD measurements under voltage pulses were conducted. In these measurements, an x-ray microbeam of less than 4 μm width was focused inside the Pt top electrodes, for which the position of x-ray was determined by detecting the characteristic x-ray emitted from Pt. 200-ns unipolar pulses of 15, 20, or 25 V were applied repeatedly at 800-ns intervals to the samples to achieve a sufficient intensity. Figure 3(a) shows the time-resolved synchrotron XRD around PZT 002 as a function of time. Irrespective of the voltage, the PZT 002 peak position shifted to a lower 2θ angle when the voltage

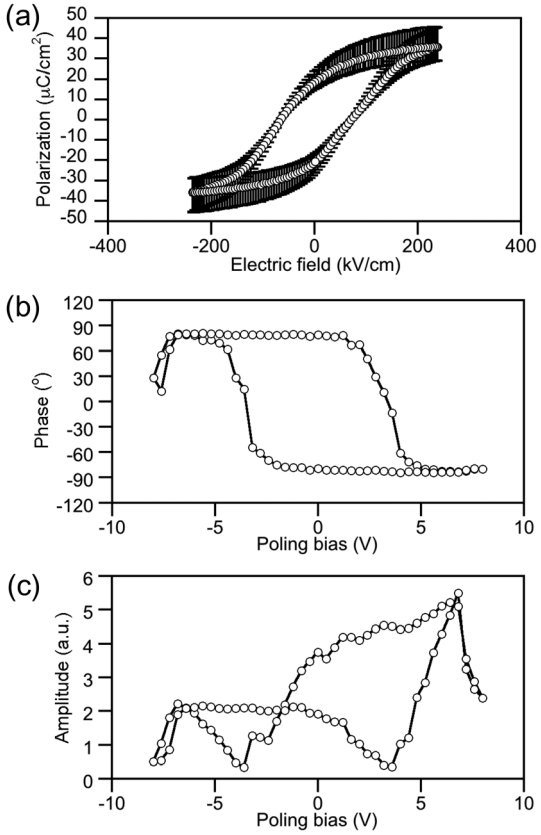

FIG. 2. Electrical and electromechanical properties of the fabricated Pb(Zr, Ti)O_3 nanorods: (a) *P-E* hysteresis loop measured by a ferroelectric tester, and (b) phase and (c) amplitude of piezoresponse measured by piezoelectric force microscopy.

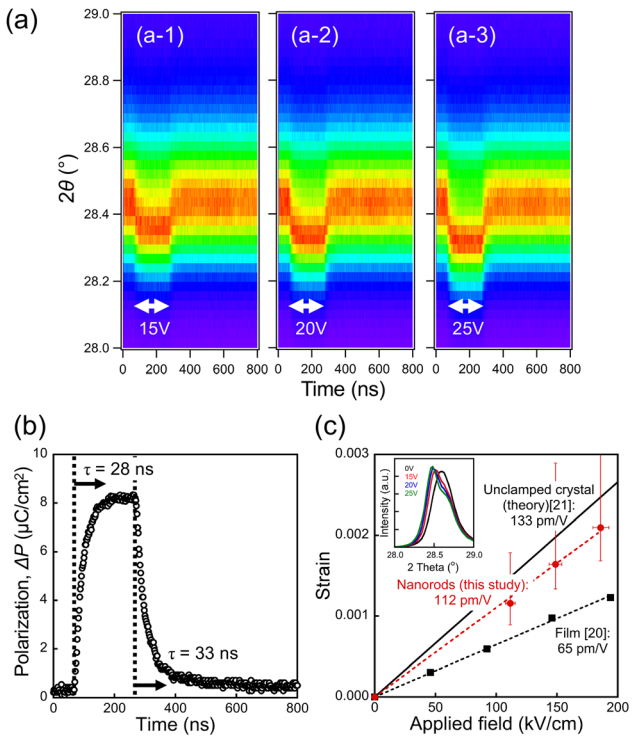

FIG. 3. Piezoelectric properties of the fabricated Pb(Zr, Ti)O_3 nanorods: (a) time-resolved synchrotron x-ray diffraction (XRD) under 200-ns-width unipolar 15, 20, and 25 V pulses; (b) change in polarization following application of a 200-ns-width unipolar 20 V pulse; and (c) field-induced strain as a function of the applied electric field and XRD peak profiles under different voltages (inset).

was applied and resumed when the voltage was removed, which indicates lattice elongation along the out-of-plane direction by the electric field. It is worth noting that there were small delays in the change in peak position from the application to removal points of the electric field. To explore the origin of these delays, the change in the polarization value by the application of 20 V is plotted in Fig. 3(b). By fitting the data using an exponential relaxation model, the delay time was estimated to be 28 ns, when voltage was applied and 33 ns, when it was removed. The observed delays are not far from the calculated value of 18 ns for a series circuit with similar top and bottom electrodes[22] and contrast with the multi-domain films that show appreciable domain switching, which exhibit a longer delay time of 95 ns for the removal of the voltage.[22] Therefore, it can be said that the observed time delay was caused by neither relaxation of the domain switching nor any other extrinsic factor; rather, the piezoelectric response of the fabricated nanorods is dominated by intrinsic contributions.

Figure 3(c) shows the XRD peak profiles under different voltages (inset) and the evaluated field dependence of the strain for the fabricated nanorods. The slope in the field dependence of the strain represents the piezoelectric constant, d_{33}. For comparison, the theoretical line for the unclamped single-domain crystal[21] and the experimental data for the single *c*-domain (001) film of the same composition and by using the same measurement system and profile as the present study[20] are also shown. Here, it should be noted that, in addition to the shift of XRD peak position, the peak profiles become to have a shoulder on the right-hand side by increasing the electric field, which might be due to the inhomogeneous electric field inside the nanorods or the influence of the initial continuous layer clamped by substrate; the further clarification is needed in the future. In order to avoid possible overestimation of the field-induced strain, the median of peaks was taken as the representative values. As can be seen, the d_{33} of the (001) films[20] was significantly lower than the theoretical value of the unclamped single-domain crystal.[21] This could have been due to the influence of the substrate clamping, expressed as $d_{33} = d_{33} - 2d_{31}s_{13}^E/\left(s_{11}^E + s_{12}^E\right)$, where s_{ij}^E is the elastic compliance.[2,3,20] On the other hand, the nanorods fabricated in this study showed a d_{33} that was 84% of the theoretical unclamped crystal and 105% higher than the substrate clamped film. As found by Chen *et al.* and Nagarajan *et al.*, the critical aspect ratio (height divided by width) for declamping depends on ferroelectric materials and substrates, but is generally 1 or less.[11,23] As described above, the aspect ratio for the most of nanorods in this study is larger than 2.9, which is sufficiently large to eliminate the substrate clamping.[23] Therefore, an intrinsic piezoelectric constant close to that of theoretical unclamped crystal[21] was achieved.

In summary, in this study, self-assembled (001)-epitaxial PZT nanorods with a *c*-domain structure were fabricated. The stabilization of *c*-domain in the nanorods can be understood by the model based on the imperfect charge screening on their sidewall. The estimated spontaneous polarization and the observed short delay time of the change in polarization when voltage was applied and removed agree with the fact of the *c*-domain structure in the nanorods. The time-resolved XRD measurements demonstrated that the large aspect ratio of the nanorods has significantly reduced substrate clamping, and the fabricated complete *c*-domain nanorods showed a piezoelectric constant close to that of unclamped single crystals.

See the supplementary material for the chemical composition analysis, the width distribution, and the detailed piezoresponse of the fabricated PZT nanorods.

This work was mainly supported by JST-PRESTO "Nanosystems and Emergent Functions" and "Scientific Innovation for Energy Harvesting Technology, Grant No. JPMJPR16R9," and partially supported by the JSPS KAKENHI Grant Nos. 26709047 (T.Y.), 15K13944 (T.Y.), 19J21955 (K.O.), 19H02421 (T.K.), and 19H04531 (T.K.). The synchrotron radiation experiments were performed at the BL13XU and BL15XU beamlines at SPring-8 with the approval of the Japan Synchrotron Radiation Research Institute (JASRI) (Proposal Nos. 2011A1550, 2012A1491, and 2016B1543) and the Synchrotron x-ray Station, NIMS (Proposal Nos. 2014A4908, 2014B4908, and 2018A4901). The authors are grateful to Dr. K. Yokoyama, Dr. S. Takeda, Professor Y. Kagoshima, and Professor J. Matsui, University of Hyogo, for their technical contribution in the BL15XU measurement. The TEM experiments were supported by Tohoku University Nanotechnology Platform Project sponsored by MEXT and the Collaborative Research Project of Laboratory for Materials and Structures, Institute of Innovative Research (11M196).

DATA AVAILABILITY

The data that support the findings of this study are available within the article and its supplementary material.

REFERENCES

[1]D. J. Kim, J. P. Maria, A. I. Kingon, and S. K. Streiffer, J. Appl. Phys. **93**, 5568 (2003).
[2]K. Lefki and G. J. M. Dormans, J. Appl. Phys. **76**, 1764 (1994).
[3]P. Muralt, J. Micromech. Microeng. **10**, 136 (2000).
[4]N. Setter, D. Damjanovic, L. Eng, G. Fox, S. Gevorgian, S. Hong, A. Kingon, H. Kohlstedt, N. Y. Park, G. B. Stephenson, I. Stolitchnov, A. K. Taganstev, D. V. Taylor, T. Yamada, and S. Streiffer, J. Appl. Phys. **100**, 51606 (2006).
[5]T. Yamada, J. Yasumoto, D. Ito, O. Sakata, Y. Imai, T. Kiguchi, T. Shiraishi, T. Shimizu, H. Funakubo, M. Yoshino, and T. Nagasaki, J. Appl. Phys. **118**, 072012 (2015).
[6]T. Fujisawa, H. Nakaki, R. Ikariyama, T. Yamada, M. Ishikawa, H. Morioka, and H. Funakubo, J. Appl. Phys. **105**, 061614 (2009).
[7]M. Nakajima, H. Nakaki, Y. Ehara, T. Yamada, K. Nishida, T. Yamamoto, M. Osada, and H. Funakubo, Appl. Phys. Lett. **97**, 181907 (2010).
[8]C. S. Ganpule, A. Stanishevsky, Q. Su, S. Aggarwal, J. Melngailis, E. Williams, and R. Ramesh, Appl. Phys. Lett. **75**, 409 (1999).
[9]S. Bühlmann, B. Dwir, J. Baborowski, and P. Muralt, Appl. Phys. Lett. **80**, 3195 (2002).
[10]V. Nagarajan, A. Roytburd, A. Stanishevsky, S. Prasertchoung, T. Zhao, L. Chen, J. Melngailis, O. Auciello, and R. Ramesh, Nat. Mater. **2**, 43 (2003).
[11]V. Nagarajan, Appl. Phys. Lett. **87**, 242905 (2005).
[12]A. Bernal, A. Tselev, S. Kalinin, and N. Bassiri-Gharb, Appl. Phys. Lett. **101**, 112901 (2012).
[13]R. Keech, L. Ye, J. L. Bosse, G. Esteves, J. Guerrier, J. L. Jones, M. A. Kuroda, B. D. Huey, and S. Trolier-McKinstry, Adv. Funct. Mater. **27**, 1605014 (2017).
[14]M. D. Nguyen, E. P. Houwman, M. Dekkers, and G. Rijnders, ACS Appl. Mater. Interfaces **9**, 9849 (2017).
[15]K. Okamoto, T. Yamada, J. Yasumoto, K. Nakamura, M. Yoshino, and T. Nagasaki, J. Ceram. Soc. Jpn. **126**, 276 (2018).

[16]T. Kamo, K. Nishida, K. Akiyama, J. Sakai, T. Katoda, and H. Funakubo, Jpn. J. Appl. Phys., Part 1 **46**, 6987 (2007).
[17]O. Sakata, S. Yasui, T. Yamada, M. Yabashi, S. Kimura, and H. Funakubo, AIP Conf. Proc. **1234**, 151 (2010).
[18]T. Yamada, D. Ito, O. Sakata, J. Kuroishi, T. Namazu, Y. Imai, T. Shiraishi, T. Shimizu, H. Funakubo, M. Yoshino, and T. Nagasaki, Jpn. J. Appl. Phys., Part 1 **54**, 10NA07 (2015).
[19]T. Yamada, D. Ito, T. Sluka, O. Sakata, H. Tanaka, H. Funakubo, T. Namazu, N. Wakiya, M. Yoshino, T. Nagasaki, and N. Setter, Sci. Rep. **7**, 5236 (2017).
[20]T. Fujisawa, Y. Ehara, S. Yasui, T. Kamo, T. Yamada, O. Sakata, and H. Funakubo, Appl. Phys. Lett. **105**, 012905 (2014).
[21]M. J. Haun, Z. Q. Zhuang, E. Furman, S. J. Jang, and L. E. Cross, Ferroelectrics **99**, 45 (1989).
[22]Y. Ehara, T. Shimizu, S. Yasui, T. Oikawa, T. Shiraishi, H. Tanaka, N. Kanenko, R. Maran, T. Yamada, Y. Imai, O. Sakata, V. Nagarajan, and H. Funakubo, Phys. Rev. B **100**, 104116 (2019).
[23]J. H. Li, L. Chen, V. Nagarajan, R. Ramesh, and A. L. Roytburd, Appl. Phys. Lett. **84**, 2626 (2004).